Environ. Sci. Technol. **2007,** *41,* 8154–8158

Sustainable Power Generation in Microbial Fuel Cells Using Bicarbonate Buffer and Proton Transfer Mechanisms

YANZHEN FAN, HONGQIANG HU, AND HONG LIU*

Department of Biological and Ecological Engineering, Oregon State University, 116 Gilmore Hall, Corvallis, Oregon 97331

Received July 13, 2007. Revised manuscript received September 11, 2007. Accepted September 19, 2007.

Phosphate buffer solution has been commonly used in MFC studies to maintain a suitable pH for electricity-generating bacteria and/or to increase the solution conductivity. However, addition of a high concentration of phosphate buffer in MFCs could be expensive, especially for wastewater treatment. In this study, the performances of MFCs with cloth electrode assemblies (CEA) were evaluated using bicarbonate buffer solutions. A maximum power density of 1550 W/m^3 (2770 mW/m^2) was obtained at a current density of 0.99 mA/cm^2 using a pH 9 bicarbonate buffer solution. Such a power density was 38.6% higher than that using a pH 7 phosphate buffer at the same concentration of 0.2 M. Based on the quantitative comparison of free proton transfer rates, diffusion rates of pH buffer species, and the current generated, a facilitated proton transfer mechanism was proposed for MFCs in the presence of the pH buffers. The excellent performance of MFCs using bicarbonate as pH buffer and proton carrier indicates that bicarbonate buffer could be served as a low-cost and effective pH buffer for practical applications, especially for wastewater treatment.

Introduction

Microbial fuel cell (MFC) technology has drawn much research attention recently due to its promising application potential in wastewater treatment and renewable energy generation (*1, 2*). Amplifying the power density is one of the greatest challenges for the practical applications of MFCs. Many efforts have been made to improve the power generation, including (i) isolation and selection of electricity-generating bacteria (*3–5*), (ii) selection and modification of electrodes (*6–9*), (iii) selection and treatment of membranes (*10–12*), and (iv) optimization of the MFC design (*13–19*). A few studies have also been reported on the effect of solution chemistry such as ionic strength (*20*) and pH (*21*) on MFC performance.

Phosphate buffer solution has been commonly used in MFC studies (*11–21*) to maintain a suitable pH for electricity-generating bacteria and/or to increase the solution conductivity. It was reported that the optimal pH was 7 for two-chamber MFCs using phosphate as buffer (*21*). In the absence of buffer, the pH in anode and cathode chambers was changed from 7 to 5.4 and 9.5, respectively, resulting in a much lower power output (*21*). While significant power increase can be achieved through increasing phosphate buffer concentration (*9*), there are two potential drawbacks using phosphate in MFCs. One is that the addition of a high concentration of phosphate buffer in MFCs is expensive, especially for the application in wastewater treatment. The other is that phosphates can contribute to the eutrophication conditions of water bodies if the effluents are discharged without the removal of phosphates. The lack of cost-effective phosphate recovery techniques makes it impractical for wastewater treatment. On the other hand, CO_2 generated from the degradation of carbon sources may serve as a low cost and effective pH buffer. However, the effect of the CO_2–bicarbonate–carbonate buffer system on the performance of MFCs has not been systematically investigated.

While pH buffer can help stabilize the solution pH and increase the solution conductivity, the roles of pH buffer in facilitating proton transfer and reducing internal resistance in MFCs have not been well studied. The proton transfer mechanism in MFC is distinct from that of chemical fuel cell due to the extremely low concentration of protons (or OH^-) at near neutral condition. A clear understanding of proton transfer mechanism is needed to estimate or calculate the effectiveness of the pH buffers and the suitable pH range in promoting the proton transfer from anode to cathode and reducing the internal resistance. Alkali ions, instead of protons, accounted for a major portion of the charge transfer in two-chamber MFCs using proton exchange membrane (PEM) (*22*). The transfer of phosphate anion species was found in two-chamber MFCs with anion exchange membrane (AEM) (*12*). For single-chamber fuel cells, however, protons must be transferred in order to form a sustainable current. Therefore, the charge/protons transfer in a single-chamber MFC system involves a totally different mechanism.

In our previous study, we reported a power density of 1010 W/m^3, the highest volumetric power density up to date, using MFCs with cloth electrode assemblies (CEAs) (*14*). The CEA configuration holds a significant meaning for future practical applications considering its high power density as well as the simple and cost-effective design. The fixed and relatively small spacing between anode and cathode in a CEA can maintain the low specific internal resistance during scale-up.

In this study, the performances of CEA MFCs using bicarbonate buffer were evaluated under continuous operation, and compared with those using phosphate buffer. The effect of pH using bicarbonate buffer on the performances of MFCs in terms of power generation and internal resistance was also investigated. The proton transfer mechanisms in the presence of pH buffers were then discussed. Quantitative comparison was made on the facilitated proton transfers by phosphate buffer and bicarbonate buffer.

Materials and Methods

CEA MFC Construction. Single-chamber air-cathode MFCs with double CEAs (cloth electrode assemblies) were constructed as previously described (*14*). Briefly, two layers of J-Cloth (Associated Brands LP) were sandwiched between the carbon cloth anode and the carbon cloth/Pt/PTFE cathode to form a CEA. Then one CEA was placed at each end of the cylindrical chamber with a diameter of 3 cm which resulted in a total empty bed volume of 2.5 mL. The photo and schematic of the CEA reactor are available in the Supporting Information (Figure S1).

CEA MFC Operation. The MFC inoculation, enrichment, and media composition were the same as previously described (*14, 23*) with the exception of pH buffer. Phosphate

* Corresponding author phone: 541-737-6309; fax: 541-737-2082; e-mail: liuh@engr.orst.edu.

10.1021/es071739c CCC: $37.00
Published on Web 11/03/2007

buffer (pH 7.0), prepared with monobasic and dibasic phosphates, was used to investigate the effect of buffer concentration (0.05, 0.1, and 0.2 M) on power generation. The performance of MFCs using bicarbonate buffer was investigated at pH 7, 8, 8.5, 9, and 9.5. The buffer was prepared with 0.2 M bicarbonate. HCl or NaOH was applied to adjust the pH value. The bicarbonate buffer in this paper refers to both carbonic acid–bicarbonate buffer ($pK_1 = 6.4$) and bicarbonate–carbonate buffer ($pK_2 = 10.3$) because bicarbonate dominates in concentration in the studied pH range.

The CEA MFCs were continuously operated in an upflow mode at a constant flow rate of 0.6 mL/min maintained through a peristaltic pump (MasterFlex 7550-10, Cole-Parmer Instrument Co.). Cell voltages at various external resistances from 7 to 1000 Ω were measured to make the polarization curves. At each resistance, MFCs ran for at least two hours to ensure stable power output had been achieved.

Analyses. Voltage (V) was recorded using a multimeter with a data acquisition system (2700, Keithly, USA), and used to calculate the volumetric power densities based on empty bed volume (2.5 mL) and surface power density based on projected surface area of electrode (14 cm^2 due to the double CEAs).

Internal resistance was analyzed by electrochemical impedance spectroscopy (EIS) using a potentiostat (G300 potentiostat, Gamry Instrument Inc.) over a frequency range of 3×10^5 to 0.005 Hz between the anode and cathode (two-electrode mode). The cathode was used as the working electrode and the anode was used as the counter and reference electrode. Impedance measurements were conducted at constant potential of 300 mV with a sinusoidal perturbation of 5 mV amplitude. Before starting each impedance measurement the MFC was operated at 300 ± 25 mV for more than 1 h then prepolarized for at least 15 min at 300 mV provided by the potentiostat to reach steady state conditions. The internal resistances of the cell were shown as Nyquist diagrams which provide a description about the internal resistance of a cell resulting from ohmic, kinetic, or transport limitations. The intercept of the curve with the Z_{re} axis was considered as the ohmic resistance and Z_{re} value of the lowest frequency was considered as the total internal resistance (*19, 24*). The difference between the total resistance and the ohmic resistance is the charge-transfer and diffusion resistance. Since the measured diffusion resistance highly depends on the applied frequency (*24*), 0.005 Hz was applied as the lowest frequency in this study to clearly show the contribution of the diffusion to internal resistance. Since the internal resistance is in reverse proportion to the electrode surface area, area-specific resistances (Ω cm^2) were also calculated by multiplying the internal resistances (Ω) with the projected electrode area (cm^2) for comparison with other studies.

Results

Power Generation Using Phosphate Buffers at pH 7. High power density has been continuously produced from acetate by the double CEA MFC for over 3 months at 30 °C. A maximum power density of 697 W/m^3 (1250 mW/m^2) was generated using 0.05 M buffer solution (Figure 1). An over 44.9% increase in power density was obtained (1010 W/m^3; 1800 mW/m^2) when the buffer concentration was increased from 0.05 to 0.1 M. Further increase of buffer concentration from 0.1 to 0.2 M resulted in an only 11% increase in power density (from 1010 to 1120 W/m^3).

Power Generation Using Bicarbonate Buffers at Various pHs. When the medium solution was switched from 0.2 M phosphate buffer (pH 7) to 0.2 M bicarbonate buffer (pH 7), a similar power density (1090 W/m^3 using biocarbonate buffer vs 1120 W/m^3 using phosphate buffer) was generated (Figure 2). Increasing the pH from 7 to 9 resulted in an over 42.2%

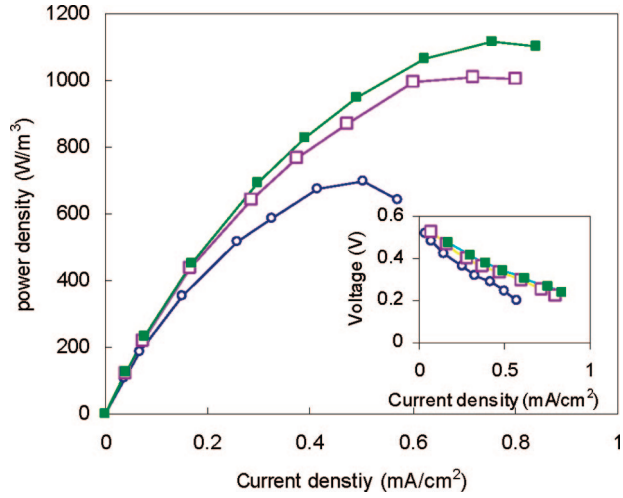

FIGURE 1. Effect of phosphate buffer strength on power and voltage generation at different current densities at pH 7 (○, 50 mM phosphate buffer; □, 100 mM phosphate buffer; ■, 200 mM phosphate buffer.)

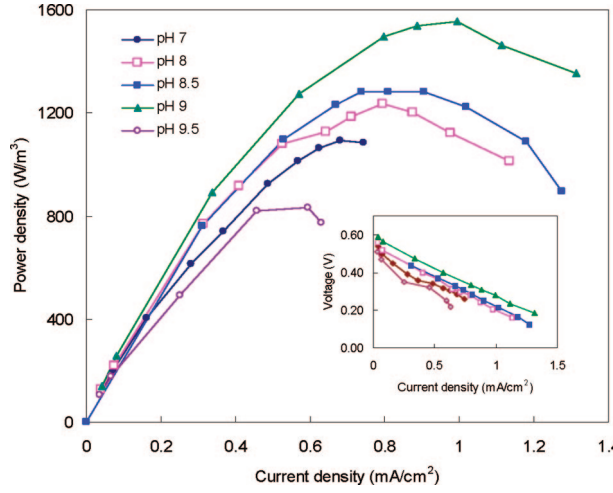

FIGURE 2. Effect of pH on power and voltage generation at different current densities with 200 mM bicarbonate buffer solution.

improvement in maximum power density, reaching 1550 W/m^3 (2770 mW/m^2) at a current density of 0.99 mA/cm^2. Further increasing the pH to 9.5, however, reduced the power density to 833 W/m^3. The performance of the MFC using bicarbonate buffer at a pH range of 8–9.5 was demonstrated in Figure 3. High power was generated immediately following the change of pH without any adaptation phase.

Internal Resistance of Cell with Bicarbonate Buffer Solutions. Ohmic resistances varied slightly for different pH values ranging from 3.5 to 4 Ω, corresponding to area-specific resistances of 49–56 Ω cm^2 (Figure 4). The charge-transfer and diffusion resistance, however, was greatly affected by the pH and decreased from 23.5 Ω (329 Ω cm^2) at pH 7 to 11.2 Ω (157 Ω cm^2) at pH 9 and then increased to 16.5 (231 Ω cm^2) when pH was further increased to 9.5. It was also demonstrated in Figure 4 that resistances resulted from charge-transfer and diffusion attributed to the major part of the total internal resistances over the pH range of 7–9.5.

Discussion

High Power Density of CEA MFCs Using a Bicarbonate Buffer. The obtained power density of 1550 W/m^3 (2770 mW/m^2) using a bicarbonate buffer (0.2 M and pH 9) is higher than the 1120 W/m^3 (1990 mW/m^2) using phosphate buffer

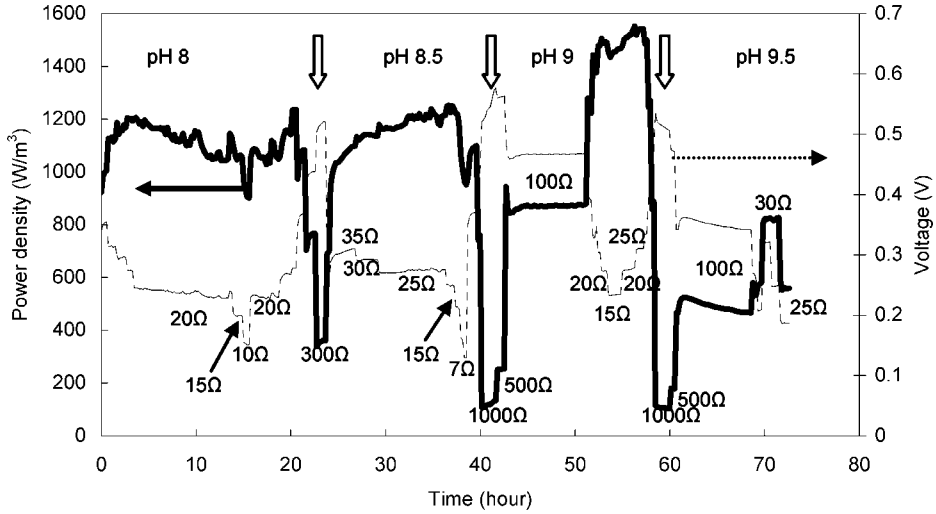

FIGURE 3. Power density (solid line) and voltage generation (dashed line) at different pHs with 0.2 M bicaronate buffer solution. Open arrows indicate the changes in pH.

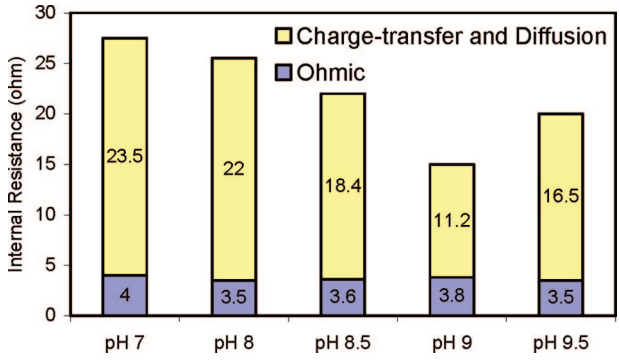

FIGURE 4. Internal resistances of the MFCs using bicarbonate buffer solution at various pHs. Total internal resistances are the sum of ohmic resistances and charge-transfer and diffusion resistance.

(0.2 M and pH 7) in this study and is more than 10 times higher than those reported previously using single-chamber air-cathode MFCs (*8, 9*). It was also 210% higher than the power density (500 W/m^3) generated from a miniature two-chamber MFC using ferricyanide as catholyte (*16*). In addition, the surface power density of 2770 mW/m^2 generated in this CEA MFC was comparable to that of air-cathode MFCs (2400 mW/m^2) using brush anode calculated based on cathode surface area (*8*) and that of two chamber miniature MFCs (3000 mW/m^2) using ferricyanide as catholyte (*16*), but lower than the 4310 mW/m^2 of MFCs using ferricyanide as catholyte (*5*).

While the high electrode surface area to reactor volume ratio of the CEA type MFCs (560 m^2/m^3) accounted for the high volumetric power density (*14*), the low internal resistance was also attributed to the high power output when bicarbonate buffer was used. The ohmic internal resistances of CEA MFCs using 0.2 M bicarbonate buffer in this study were 3.5–4 Ω, corresponding to a specific resistance of 49–56 Ω cm^2. Such a specific ohmic resistance is comparable to the 3.9 Ω (55 Ω cm^2) of CEA MFCs using 0.1 M phosphate buffer (*14*) and the 56 Ω cm^2 (based on the cathode projected area of 7 cm^2) of the brush-anode MFC using 0.2 M phosphate buffer (*8*), but lower than the 112 and 245 Ω cm^2 of a similar air-cathode MFC using 0.05 M phosphate buffer with an electrode spacing of 1 and 2 cm, respectively (*13*). It is only about 3% of the 1620 Ω cm^2 of an upflow reactor, which was calculated based on membrane surface area (*19*). The lower specific ohmic resistance obtained in this study was due to the special reactor configuration, where the cloth layers in

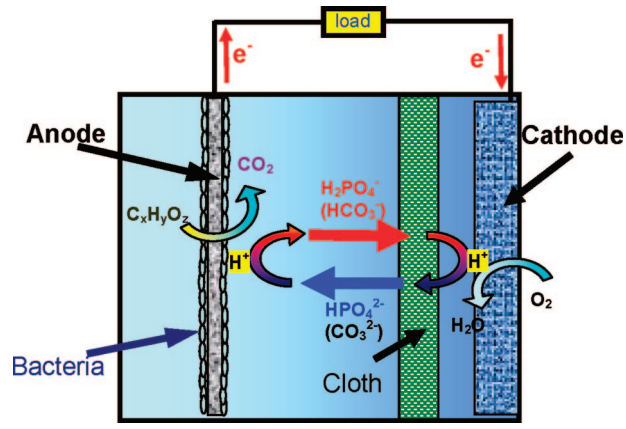

FIGURE 5. Diagram of proton transfer mechanism in air cathode MFCs with a cloth/membrane layer. The monobasic phosphate/dibasic phosphate ion-pair accounts for the major mechanism for protons transfer in air cathode MFCs using phosphate buffer, while bicarbonate-carbonate is the major proton carrier for MFCs using bicarbonate buffer.

CEA MFCs can significantly reduce the oxygen diffusion through the air cathode, making it possible to greatly decrease the electrode spacing and form a CEA structure (*14*). The reduction of electrode spacing and the change of solution chemistry could also result in the reduction of charge-transfer and diffusion resistance, which was the major part of the total internal resistance (Figure 5), and attribute to the enhanced power generation.

Proton Transfer Mechanisms in the Presence of pH Buffers. To generate a sustainable current, the proton generated on the anode must be transferred to the cathode in a single-chamber MFC system. To investigate the role of pH buffer in facilitating proton transfer and reducing internal resistance in MFCs, the possible proton transfer mechanisms were discussed as below.

Similar to the charge transfer in a common battery or electrolyzer (*25*), there are three mechanisms for the transfer of protons from anodes to cathodes in single-chamber MFCs: (1) convection: proton transfer through mechanical motion of the electrolyte; (2) electric migration: proton transfer through an electric field, i.e., an electrical potential gradient; (3) diffusion: proton transfer through a chemical potential gradient, i.e., a concentration gradient.

For the MFCs studied here, convection played a neglible role in proton transfer because there was no stirring or

vibration. The small anode and cathode spacing for CEA also prevented the occurrence of natural convention.

Protons can be transferred via electric migration in an electric field. The transference number of proton, t_p (unitless), or the fraction of the total current that proton carries, can be computed as (*25*)

$$t_p = \frac{C_p \lambda_p}{\sum_j |z_j| C_j \lambda_j} \quad (1)$$

where C_p and C_j are the concentrations of proton and ion j, respectively; λ_p and λ_j are the molar ionic conductivities for proton and ion j, respectively; and z_j is the charge on ion j.

For MFCs using 0.1 M phosphate buffer, the fraction of the current that proton carried (t_p) was less than 2×10^{-6} because of the comparable molar ionic conductivities of ions (*26*) and the much lower concentration of proton (10^{-7} M at pH 7) than those of other ions, such as Na^+ (0.161 M), HPO_4^{2-} (0.061 M), and $H_2PO_4^-$ (0.039 M). Therefore, the electric migration of free protons is also negligible.

The diffusion rate of protons (W) can be calculated through Fick's Law (equation 2)

$$W = -DA\Delta C/\delta_m \quad (2)$$

where D is the diffusion coefficient of protons in the cloth, 9.3×10^{-5} cm^2 s^{-1} in water at 30 °C (*27*); δ_m is the cloth thickness (two layers of J-Cloth is about 0.6 mm); A is the cross-sectional area (14 cm^2); and ΔC is the concentration difference. According to eq 2, the diffusion of free protons is very ineffective because of the extremely low anodic and cathodic proton concentration difference ($\Delta C < 10^{-7}$ M at pH 7). The maximum diffusion rate of protons through a 0.6 mm (the thickness of two layers of J-Cloth) pure water layer is 7.8×10^{-6} mmol h^{-1}. The maximum current in the studied MFCs was about 20 mA, corresponding to a proton transfer rate of 0.75 mmol h^{-1}, which is about 10^5 times higher the maximum diffusion rate of free protons, indicating that the diffusion of free protons is also negligible.

Therefore, the majority of protons were transferred neither by the diffusion, nor by the electric migration of free protons. There must be some proton carriers that facilitate the proton transfer. The only carriers for the facilitated proton transfer are proton carriers, i.e., pH buffers.

Monobasic and dibasic phosphates, carrying dissociable protons, were commonly used in MFCs as pH buffer at a much higher concentration (0.05–0.2 M in this study) than free protons. In spite of the fact that the diffusion coefficients of monobasic and dibasic phosphate (1.0×10^{-5} and 0.86×10^{-5} cm^2 s^{-1} at 30 °C (*28*)) are about ten times lower than that of free protons, the mediated transfer of protons by phosphate ions diffusion could be about 10^5 times more effective than free diffusion of protons due to the much higher possible concentration difference ($\Delta C < 0.1$ M). According to eq 2, the maximum proton flux from anode to cathode via monobasic phosphate (0.1 M phosphate buffer) through a 0.6 mm × 14 cm^2 J-Cloth layer is about 0.84 mmol h^{-1}, corresponding to a current of 22 mA, which is about two times the maximum current in the MFCs using phosphate buffer (12 mA). This indicates that phosphate ions might be the major carrying ions for proton transfer in the studied MFCs using phosphate buffer. Figure 5 demonstrates such a mechanism for proton transfer in MFCs. The protons produced at the anode react rapidly with dibasic phosphate to form monobasic phosphate. The latter diffuses from anode to cathode, releases proton to cathode, and then transfers back to anode as dibasic phosphate via diffusion and electric migration.

The mechanism is also suitable for other MFC systems with the exception of MFCs with cation exchange membrane, in which the charges are mainly transferred by cations other than proton. The mechanism of the facilitated proton transfer explains the reason that the increase in the concentration of phosphate buffer is so effective in the increase of the power density. The increase of phosphate concentration can increase the diffusion rate and electric migration rate of proton carriers, i.e., monobasic and dibasic phosphates, since both rates are concentration-dependent. The increased proton transfer rate reduces the internal resistance caused by proton concentration polarization, enhancing the power output. This was supported by the 60% increase in power density, from 697 to 1115 W/m^3, when the concentration of phosphate buffer increased from 0.05 to 0.2 M.

Bicarbonate as pH Buffer and Proton Carrier. The facilitated proton transfer mechanism can help to explain the reason that the power density of MFCs using 0.2 M bicarbonate buffer was higher at pH 9 than at pH 7. The maximum proton transfer rate via bicarbonate depends on its concentration and the CO_2 solubility, which in turn depends on the solution pH and CO_2 partial pressure. For a 0.2 M bicarbonate solution, the CO_2 partial pressure is high at pH 7 (0.7 atm), which could result in a slow release of CO_2 through the cathode since the waterproofing PTFE coating on the cathode is gas permeable. The release of CO_2 could decrease the bicarbonate availability for proton transfer. At pH 9, the CO_2 partial pressure is much lower (0.005 atm), slowing down the CO_2 loss. The increased bicarbonate concentration might be the major reason for the reduced internal resistance and increased power density of MFCs at pH 9.

Solution pH might also affect bacterial community and metabolism. Our preliminary study showed that the power density generated using a 0.2 M phosphate buffer solution at pH 9 (500–600 W/m^3) was lower than that using a pH 7 solution. This is also consistent with a previous report that MFCs using phosphate buffer produced the highest power at pH 7 (*21*). The power density was also much lower than that using bicarbonate buffer at the same pH. Therefore, the pH difference is not reason for the high power density using a pH 9 bicarbonate buffer in this study. It also indicates that the anode reaction catalyzed by bacteria might not be the limiting factor for the tested MFCs with pH values less than 9. At pH 9.5, however, the microbial anode reaction might limit the power generation, as indicated by the greatly decreased power density but only slightly increased internal resistance.

The facilitated proton transfer mechanism can also help to explain why MFCs using bicarbonate buffer produced more power than those using phosphate buffer at same concentration. The proton transfer rate via bicarbonate is about 34% higher than that of monobasic phosphate due to the higher mass transfer coefficient of bicarbonate in water (1.34×10^{-5} cm^2/s vs 1.0×10^{-5} cm^2/s at 30 °C, (*29*)). The higher diffusion rate of protons carried by bicarbonate resulted in a decreased internal resistance and increased power density. At the same concentration of 0.2 M, MFCs with bicarbonate at pH 9 achieved 38.6% higher power generation than those with phosphate solution at pH 7. Another possible reason for the higher power density generated by using biocarbonate is that the relatively small bicarbonate ions can carry protons to some catalytic sites in the cathodes that are not accessible for the relatively big monobasic or dibasic phosphate ions.

Implications in MFC Applications. The excellent performance of MFCs using bicarbonate as pH buffer and proton carrier indicates that bicarbonate might be more practical than phosphate buffer, especially for wastewater treatment. Bicarbonate is cheaper than phosphate. Another great advantage of bicarbonate buffer is that it can be converted from the self-produced CO_2 in a MFC. Although carbonate or base may still be needed to adjust the pH, the accumulation

of CO_2 in a half-closed or closed MFC system may reduce or eliminate the need for the addition of buffers, making such a MFC system simpler and more economically viable. The mechanism of facilitated proton transfer creates a new avenue of research for MFC design and operation, membrane and electrodes development. The contribution of the produced CO_2 on the internal resistance and power generation of MFCs needs to be considered in future study, especially for the MFCs with low concentration of other buffers. Effective design and operation of MFCs may enhance the concentration of bicarbonate in the MFCs, thus lower the internal resistance and increase the power density. The membranes and electrodes developed for chemical fuel cells may be not suitable for MFCs because of the totally different proton transfer mechanism. New membrane and electrode materials need to be developed with the consideration of the mass transfer of proton carriers, instead of free proton itself.

Acknowledgments

This research was partially supported by the Agricultural Research Foundation and Oregon State University General Research Fund. We acknowledge Dr. Bruce Logan for his valuable comments.

Supporting Information Available

Photo and schematic of the CEA reactor. This material is available free of charge via the Internet at http://pubs.acs.org.

Literature Cited

(1) Logan, B. E.; Hamelers, B.; Rozendal, R.; Schroder, U.; Keller, J.; Freguia, S.; Aelterman, P.; Verstraete, W.; Rabaey, K. Microbial fuel cells: methodology and technology. *Environ. Sci. Technol.* **2006**, *40*, 5181–5192.

(2) Rabaey, K.; Verstraete, W. Microbial fuel cells: novel biotechnology for energy generation. *Trends Biotechnol.* **2005**, *23*, 291–298.

(3) Bond, D. R.; Lovley, D. R. Electricity Production by *Geobacter sulfurreducens* Attached to Electrodes. *Appl. Environ. Microbiol.* **2003**, *69*, 1548–1555.

(4) Rabaey, K.; Boon, N.; Hö fte, M.; Verstraete, W. Microbial phenazine production enhances electron transfer in biofuel cells. *Environ. Sci. Technol.* **2005**, *39*, 3401–3408.

(5) Rabaey, K.; Boon, N.; Siciliano, S. D.; Verhaege, M.; Verstraete, W. Biofuel cells select for microbial consortia that self-mediate electron transfer. *Appl. Environ. Microbiol.* **2004**, *70*, 5373–5382.

(6) Park, D. H.; Zeikus, J. G. Improved fuel cell and electrode designs for producing electricity from microbial degradation. *Biotechnol. Bioeng.* **2003**, *81*, 348–355.

(7) Cheng, S.; Liu, H.; Logan, B. E. Increased power and Coulombic efficiency of single-chamber microbial fuel cells through an improved cathode structure. *Electrochem. Commun.* **2006**, *8*, 489–494.

(8) Logan, B.; Cheng, S.; Watson, V.; Estadt, G. Graphite Fiber Brush Anodes for Increased Power Production in Air-Cathode Microbial Fuel Cells. *Environ. Sci. Technol.* **2007**, *41*, 3341–3346.

(9) Cheng, S.; Logan, B. E. Ammonia treatment of carbon cloth anodes to enhance power generation of microbial fuel cell. *Electrochem. Commun.* **2007**, *9*, 492–496.

(10) Heijne, A. T.; Hamelers, H. V. M.; Wilde, V. D.; Rozendal, R. A.; Buisman, C. J. N. A bipolar membrane combined with ferric iron reduction as an efficient cathode system in microbial fuel cells. *Environ. Sci. Technol.* **2006**, *40*, 5200–5205.

(11) Biffinger, J. C.; Ray, R.; Little, B.; Ringeisen, B. R. Diversifying biological fuel cell design by use of nanoporous filters. *Environ. Sci. Technol.* **2007**, *41*, 1444–1449.

(12) Kim, J. R.; Oh, S. E.; Cheng, S.; Logan, B. E. Power generation using different cation, anion and ultrafiltration membranes in microbial fuel cells. *Environ. Sci. Technol.* **2007**, *41*, 1004–1009.

(13) Cheng, S.; Liu, H.; Logan, B. E. Increased power generation in a continuous flow MFC with advective flow through the porous anode and reduced electrode spacing. *Environ. Sci. Technol.* **2006**, *40*, 2426–2432.

(14) Fan, Y.; Hu, H.; Liu, H. Enhanced columbic efficiency and power density of air-cathode microbial fuel cells with an improved cell configuration. *J. Power Sources* **2007**, *171*, 348–354.

(15) Zuo, Y.; Cheng, S.; Call, D.; Logan, B. E. Tubular membrane cathode for scalable power generation in microbial fuel cells. *Environ. Sci. Technol.* **2007**, *41*, 3347–3353.

(16) Ringeisen, B. R.; Henderson, E.; Wu, P. K.; Pietron, J.; Ray, R.; Little, B.; Biffinger, J. C.; Jones-Meehan, J. M. High power denstity from a miniature microbial fuel cell using *Shewanella oneidensis* DSP 10. *Environ. Sci. Technol.* **2006**, *40*, 2629–2634.

(17) Aelterman, P.; Rabaey, K.; Pham, T. H.; Boon, N.; Verstraete, W. Continuous electricity generation at high voltages and currents using stacked microbial fuel cells. *Environ. Sci. Technol.* **2006**, *40*, 3388–3394.

(18) Liu, H.; Logan, B. E. Electricity generation using an air-cathode single chamber microbial fuel cell in the presence and absence of a proton exchange membrane. *Environ. Sci. Technol.* **2004**, *38*, 4040–4046.

(19) He, Z.; Wagner, N.; Minteer, S. D.; Angenent, L. T. An upflow microbial fuel cell with an interior cathode: assessment of the internal resistance by impedance spectroscopy. *Environ. Sci. Technol.* **2006**, *40*, 5212–5217.

(20) Liu, H.; Cheng, S.; Logan, B. E. Power Generation in Fed-Batch Microbial Fuel Cells as a Function of Ionic Strength, Temperature, and Reactor. *Environ. Sci. Technol.* **2005**, *39*, 5488–5493.

(21) Gil, G. C.; Chang, I. S.; Kim, B. H.; Kim, M.; Jang, J. K.; Park, H. S.; Kim, H. J. Operational parameters affecting the performance of a mediator-less microbial fuel cell. *Biosens. Bioelectron.* **2003**, *18*, 327–334.

(22) Rozendal, R. A.; Hamelers, H. V. M.; Buisman, C. J. N. Effects of membrane cation transport on pH and microbial fuel cell performance. *Environ. Sci. Technol.* **2006**, *40*, 5206–5211.

(23) Lovley, D. R.; Phillips, E. J. P. Novel mode of microbial energy metabolism: organic carbon oxidation coupled to dissimilatory reduction of iron or manganese. *Appl. Environ. Microbiol.* **1988**, *54*, 1472–1480.

(24) Wagner, N. Characterization of membrane electrode assemblies in polymer electrolyte fuel cells using a.c. impedance spectroscopy. *J. Appl. Electrochem.* **2002**, *32*, 859–863.

(25) Rieger, P. H. *Electrochemistry*, 2nd ed.; Chapman & Hall: New York, 2001.

(26) Bard, A. J.; Faulkner, L. R. *Electrochemical Methods*, 2nd ed.; John Wiley and Sons, Inc: New York, 1994.

(27) Gutman, M.; Nachliel, E.; Kiryati, S. Dynamic studies of proton diffusion in mesoscopic heterogeneous matrix. II. The interbilayer space between phospholipid membranes. *Biophys. J.* **1992**, *63*, 281–290.

(28) Mason, C. M.; Culvern, J. B. Electrical conductivity of orthophosphoric acid and of sodium and potassium dihydrogen phosphates at 25 °C. *J. Am. Chem. Soc.* **1949**, *71*, 2387–2393.

(29) Robinson, R. A.; Stokes, R. H. *Electrolyte Solutions*; Academic Press, Ltd.: London, 1959.

ES071739C